Pol. J. Environ. Stud. Vol. 32, No. 3 (2023), 2373-2381
DOI: *10.15244/pjoes/159080* ONLINE PUBLICATION DATE: 2023-03-10

Original Research

Enhanced Adsorption of Two Reactive Dyes onto Al-Based Waterworks Sludge Modified by Calcination

Minghua Wei[1,2], Xiaohan Duan[3], Wani Zhou[4], Kai Huang[4], Yawei Chen[4], Jingxi Tie[5]*

[1] School of Water Resources, North China University of Water Resources and Electric Power, Zhengzhou 450046, PR China
[2]Henan Key Laboratory of Water Resources Conservation and Intensive Utilization in the Yellow River Basin, Zhengzhou 450046, PR China
[3]School of Water conservancy, North China University of Water Resources and Electric Power, Zhengzhou 450046, PR China
[4]Zhongzhou Water Holding Co., Ltd., Zhengzhou 450000, PR China
[5]School of Environmental and Municipal Engineering, North China University of Water Resources and Electric Power, Zhengzhou 450045, PR China

Received: 19 October 2022
Accepted: 7 January 2023

Abstract

Al-based waterworks sludge (ABWS) modified by calcination was reused as an adsorbent for the removal two reactive dyes, namely, reactive yellow 176 (RY-176) and reactive red 195 (RR-195) from aqueous solution. 800ºC was proved to be the optimal calcination temperature in the range of 200-900ºC. A series of static adsorption experiments were carried out using ABWS calcinated at 800ºC (ABWS-800) as adsorbent. The results indicated that the adsorption of both the two dyes by ABWS-800 was almost independent of initial solution pH, and the adsorption capacity of ABWS-800 for RR-195 was about 1.4 times higher than that for RY-176. The pseudo-second-order kinetic model was best among the three models to describe the adsorption of the two reactive dyes, and Freundlich isotherm model was better matched than the Langmuir isotherm model to describe the adsorption process. Na_2SO4 inhibited the adsorption of the two dyes onto ABWS-800. This work provided the theoretical basis and technical support for the optimization of reaction conditions for the decontamination of dyes wastewater by "waste" ABWS.

Keywords: adsorption, reactive dye, Al-based waterworks sludge, calcination

*e-mail: 15202843@qq.com

Introduction

One of the most pressing environmental and public health challenges today is the contamination of aquatic environment by colors derived from various industrial processes, such as textile, dyeing, paper, pulp, tannery, paint, and dye manufacture, especially for those with synthetic origins [1]. Reactive dyes, which can form covalent bonds with the hydroxyl or amine groups of natural fibers, are one of the most prominent types of azo dye with various reactive groups and have a wide industrial application due to their excellent dyeing processes, brighter colors, and low price [2-4]. However, due to the high solubility of the dyes, around 10-20% of the total consumption is lost in the effluent during the dyeing process [5]. Becuse of the complex aromatic molecular structures and xenobiotic properties, they are mutagenic, carcinogenic and resistant to the physicochemical, thermal, and optical degradation in the environment [6, 7].

As a result, the dyes discharges into receiving water bodies could cause major threat to ecosystem through blocking the sunlight, reducing photosynthesis and dissolved oxygen concentration. Reactive dyes are more recalcitrant compounds than other dyes because of their defects such as strong color, high alkalinity, and high concentration of organic materials [8]. The presence of those dyes in water is highly undesirable even in very low concentrations.

Various physical, chemical, and biological technologies including coagulation/flocculation [9, 10], adsorption [11-13], advanced oxidation [14], membrane separation [15] and microbial degradation [16], etc. had been developed for reactive dye removal from water. Among those methods, adsorption had been adopted widely due to their easy operation, low cost, high efficiency and the applicability to large variety of contaminants [17-24]. Various adsorbents can be used for dyes removal from water [25-28].

As a raw material with huge potential for beneficial reuse in water and environmental engineering, waterworks sludge has been applied for the treatment of contaminants such as phosphorus [29, 30], heavy metal [31, 32], dyes [33] and so on, but the removal of reactive dyes by raw waterworks sludge was poor [33]. The adsorption performance of waterworks sludge could be improved by calcination. For instance, Jeon et al. found that the adsorption capacity of modified alum sludge for As(V) was 5.4-8.7 times greater than that of the raw adsorbent [34]. Everaert et al. revealed that the alum sludge granule calcinated at 550ºC had the largest phosphorus adsorption of 7.27 mg/g compared to those calcinated at 100ºC and 300ºC [35]. However, the research on reactive dyes adsorption by thermally modified Al-based waterworks sludge (ABWS) was currently not well documented.

Thus, the aim of this study was to evaluate the adsorption capacity of ABWS modified by calcination to remove two kinds of reactive dyes, namely, reactive yellow 176 (RY-176)and reactive red 195 (RR-195) from artificial dye-bearing wastewater. The molecular structures of the two dyes are shown in Fig. 1. Compared with RY-176, RR-195 has more anionic groups ($-SO_3^{2-}$) and larger molecular size. The physiochemical and properties of the adsorbents were characterized using X-ray florescence (XRF), X-ray diffraction (XRD), and Brunauer-Emmett-Teller surface analysis (BET). The effect of various parameters such as calcination temperature, solution initial pH, inorganic salt, and the kinetic and isotherm of adsorption process were investigated in detail.

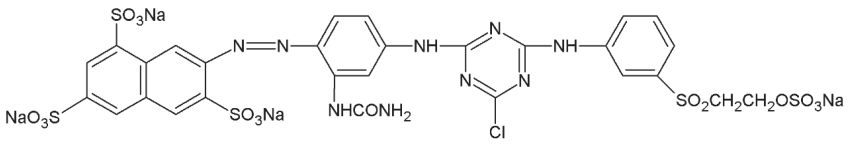

C.I. Reactive Yellow 176

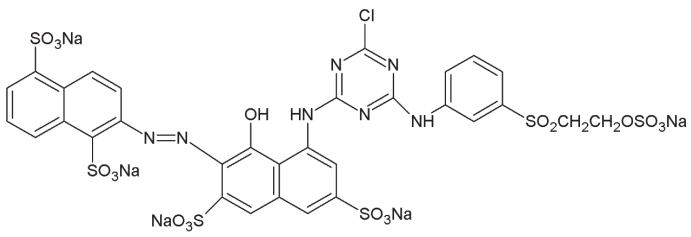

C.I. Reactive Red 195

Fig. 1. The molecular structures of RY-176 and RR-195.

Material and Methods

Calcination of the ABWS

ABWS was collected from a sludge drying filed in a drinking water treatment plant in Zhengzhou, China, where polyaluminum chloride was used as coagulant for drinking water process. ABWS collected from five points distributed at the for corners and the midpoint of the sludge drying filed was mixed evenly and dried in open air and in a drier at 105ºC for 2 h in sequence. The dried ABWS was crushed and passed through 0.15 mm screen. Then the ABWS powder was calcinated at the temperature ranging from 200ºC to 900ºC for 2 h at a temperature gradient of 100ºC. At last the ABWS calcinated at different temperature were collected to test the adsorption capacity for RY-176 and RR-195.

Characterization of ABWS

The raw ABWS and the ABWS calcinated at 800ºC (ABWS-800) which was tested to possess the best adsorption capacity for the two dyes were characterized. The X-ray florescence (XRF, Smartlab 3kw, Rigaku Ltd., Japan) was used to analyze the compositions of the two samples. XRD patterns of the two samples were obtained using an X-ray diffractometer (Smartlab 3 kw, Rigaku Ltd., Japan). The surface areas of the two samples were measured using N_2 adsorption isotherm with a model of Brunauer, Emmett, and Teller (Autosorb-I, Quantachrome, USA).

Preparation of the Artificial Wastewater

The dye-bearing wastewater was synthesized by adding RY-176 (Decai pigment chemical Co., Ltd, Shenzhen, China) and RR-195 (Yien chemical technology Co., Ltd, Shanghai, China) into the deionized water, and the pH value of the wastewater was adjusted using 0.1 mol/L HCl (Tongjie chemical reagent Co., Ltd, Shanxi, China) and NaOH (Kemio chemical reagent Co., Ltd, Tianjin, China) solutions. All of the chemicals used in this study are analytically pure.

Adsorption Experiments

Static adsorption experiments were carried out in the following way: 0.1 g ABWS and 30 mL dye-bearing solution were added into flask and allowed to react in a shaker at different temperature for various time. At the end of the reaction, the mixture was centrifugated at 8000 rpm for 5 min. The residual RY-176 and RR-195 in the supernatant were determined using a spectrophotometer (UV-5100B, Yuanxi instrument, China) at 400 nm and 540 nm, respectively. The dye uptake was calculated using the following equation [36]:

$$q = \frac{(C_0 - C_e)V}{m} \quad (1)$$

where q is the amount of RY-176 and RR-195 adsorbed (mg/g) by per unit of adsorbent, C_0 and C_e are the initial and equilibrium concentration of RY-176 and RR-195 (mg/L), respectively, V is the volume of solution (L), and m is the mass of ABWS-800 (g) used in the experiment.

Results and Discussion

Effect of Calcination Temperature

The effect of calcination temperature on the adsorption of RY-176 and RR-195 by ABWS is shown in Fig. 2.

It can be seen that the adsorption capacity o f RY-176 and RR-195 by ABWS could be changed obviously by calcination. The best removal of both the two dyes was achieved using ABWS-800, and the corresponding removal efficiency of RY-176 and RR-195 were 68.9% and 78.6%, respectively. With the further increase of calcination temperature to 900ºC, the adsorption of RY-176 and RR-195 decreased, probably resulted from the transformation of amorphous aluminum hydroxide/oxide into crystalline forms at higher calcination temperature, which would lead to the decrease of adsorption capacity [34]. Thus, 800ºC was determined to be the best calcination temperature, and ABWS-800 was used as the adsorbent in the following experiments.

Characterization of ABWS

The primary compositions of raw ABWS and ABWS-800 are shown in Table 1. SiO_2, CaO, Al_2O_3

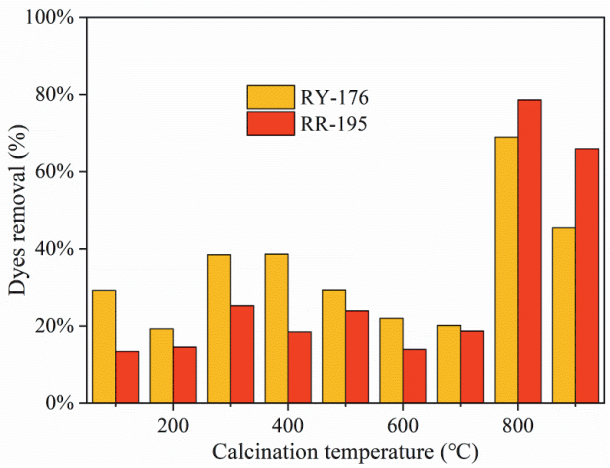

Fig. 2. Effect of calcination temperature on the adsorption of RY-176 and RR-195 by ABWS.

Table 1. The main compositions of raw ABWS and ABWS-800.

Composition	Percentage (%)	
	Raw ABWS	ABWS-800
SiO_2	40.04	39.28
CaO	34.14	35.89
Al_2O_3	10.8	10.76
Fe_2O_3	10.53	9.54
K_2O	1.21	1.19
MgO	1.14	1.33
TiO_2	0.688	0.619
Na_2O	0.293	0.309

and Fe_2O_3 were the major components of both raw ABWS and ABWS-800. SiO_2, CaO and Fe_2O_3 mainly derived from the minerals in the raw water, and Al_2O_3 might come from both the raw water and the coagulant used in the water plant. There was negligible difference between the primary composition of raw ABWS and ABWS-800, indicating that thermal treatment could hardly change the component content of the ABWS. However, unlike the results reported in the literature [34], the specific surface area decreased from 13.765 g/m^2 for ABWS to 8.378 g/m^2 for ABWS-800, which might be attributed to the destruction of the pores during the thermal treatment.

XRD analysis was conducted to determinate the crystalline structure of ABWS and ABWS-800 (Fig. 3). The XRD spectra showed that both ABWS and ABWS-800 were characterized by amorphous substances. The 2θ peaks found at 26.4° and 20.6° were assigned to SiO_2 (JSPDS 05-0492) [37] and $AlPO_4$ (JSPDS 11-0500) [38] for both ABWS and ABWS-800. The diffraction peaks presented at 29.4°, 36.0°, 39.4° and 43.17° were corresponded to $CaCO_3$ (JSPDS 47-1743) for ABWS [39, 40], which disappeared in the spectrum of ABWS-800, indicating the decomposition of $CaCO_3$ at 800ºC.

Effect of Initial Solution pH

Solution pH is an important factor for the adsorption process due to its influence on both the characteristic of adsorbent surface and ionization of dyestuff molecule [32]. The effect of initial solution pH on the adsorption of RY-176 and RR-195 on ABWS-800 was examined in the pH range of 3-10, the results are shown in Fig. 4.

As shown in Fig. 4, the adsorption capacity of RY-176 and RR-195 on ABWS-800 varied slightly as solution pH increased from 3 to 10, with a value from 12.4 mg/g to 13.5 mg/g and 17.1 mg/g to 18.3 mg/g, respectively, indicating that the adsorption of RY-176 and RR-195 on ABWS-800 was broadly independent of solution pH. The result in the present research was consistent with that reported in the literature. Kayranli et al. found that changing the pH value affected slightly on the removal of reactive blue 29 onto iron based waterworks sludge [32], and Netpradit et al. observed that when the initial pH of the dye solution was in the range 3-10, the adsorption of azo reactive dyes by metal hydroxide sludge derived from the electroplating sector was unaffected [41]. Though the adsorption of anion dyes was mainly through electrostatic attraction between sulfonate ions ($-SO_3^{2-}$) and the positive binding sites on metal hydroxide sludge, which depended highly on the pH of solution, the sludge might contain some buffer that could resist the pH change of the aqueous system to maintain a stable removal of dyes. The results of the present work implied that ABWS-800 could be applied to the removal of RY-176 and RR-195 in a wide range of initial solution pH.

In comparison, the adsorption capacity of ABWS-800 for RR-195 was about 1.4 times higher than that for RY-176, probably resulting from the fact that

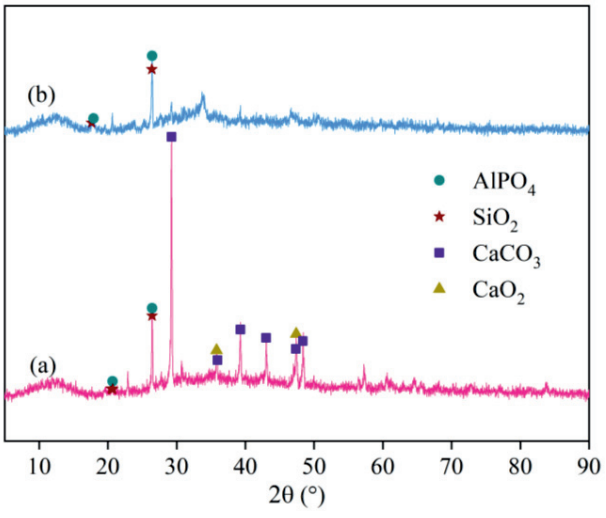

Fig. 3. The XRD pattern of the raw ABWS and ABWS-800. a) ABWS; b) ABWS-800.

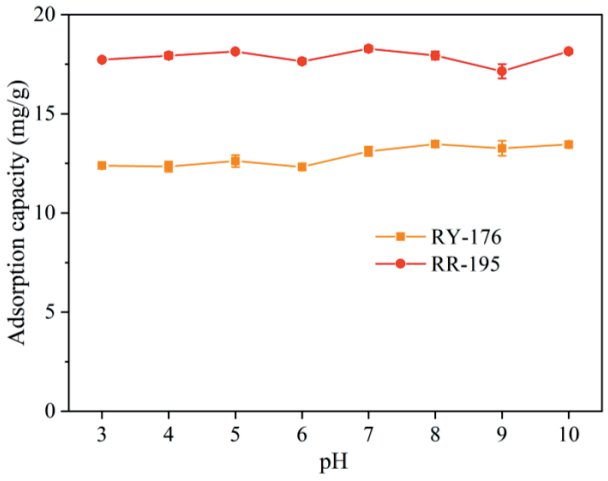

Fig. 4. Effect of initial solution pH on adsorption of RY-176 and RR-195 on ABWS-800 (Temperature: 30ºC, Reaction time: 3 h).

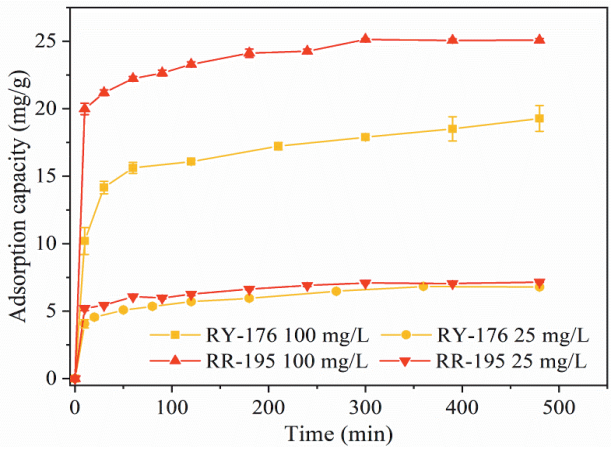

Fig. 5. The adsorption kinetic behavior of RY-176 and RR-195 onto ABWS-800 (Temperature: 30ºC, pH: 5.5).

RR-195, whose molecule was larger than RY-176, was more strongly adsorbed by metal hydroxide sludge due to its higher negative charge and lower solubility. It was concluded that more charged dyes had a higher adsorption affinity, and so the higher the charge quantity of the dyes, the greater the adsorption on the metal hydroxides sludge [42].

Kinetics Study

The kinetic behavior of the adsorption process of RY-176 and RR-195 onto ABWS-800 was examined at different dyes concentration, the result is shown in Fig. 5. The adsorption process achieved equilibrium in around 8 hours, and the equilibrium duration increased with starting dye concentration. Each of the four adsorption processes included a fast and a slow adsorption stage. The fast stage lasted from the beginning of the experiment to the 10th min during which the ABWS-800 could offer enough active sites for the adsorption reaction and resulted in a rapid adsorption. It also indicated a high affinity between the two dyes and the surface of ABWS-800. Whereas, the adsorption slowed down in the second stage, suggesting a gradual equilibrium of adsorption, probably due to less active site left for the reaction and the lagging intraparticle diffusion of the dye molecules in the adsorbent.

Three famous models, namely, pseudo-first order, pseudo-second order and Elovich model were used to fit the experiment data to further understand the adsorption process. The linear forms of the three models are presented as Eq. (2)-Eq. (4) [26]:

$$\log(q_e - q_t) = \log q_e - \frac{k_1}{2.303}t \quad (2)$$

$$\frac{t}{q_t} = \frac{t}{q_e} + \frac{1}{k_2 q_e^2} \quad (3)$$

$$q_t = \frac{1}{\beta}\ln(\alpha\beta) + \frac{1}{\beta}\ln t \quad (4)$$

where q_e (mg/g) and q_t (mg/g) are the concentration at equilibrium and time t, respectively. k_1 (1/min) and k_2 (1/min) are the pseudo-first order and pseudo-second order rate constants. α (mg/g·min) is the initial adsorption rate, and β (g/mg) is the desorption constant.

The kinetics parameters obtained from the three equations are shown in Table 2. The values of the correlation coefficient R^2 of the pseudo-second-order model were higher than those of the other two equations. Meanwhile, as shown in Table 2, the $q_{e,exp}$ obtained from the experiment of the pseudo-second-order model agreed very well with those obtained from the model. Hence, the pseudo-second-order model was the best one to describe the adsorption process, indicating that chemical adsorption was the rate controlling step and the occupancy rate of the active sites was proportional to the square of the number of unoccupied sites, the adsorption occurred via covalent bonding and ion exchange between the dyes molecule and the surface active sites of the adsorbent [43, 44]. It could be seen in Table 2 that the q_e value of RY-176 and RR-195 increased with the initial dye concentration, resulting from the larger adsorption driving force at higher adsorbate concentration.

Isotherm Study

The influence of equilibrium concentration of RY-176 and RR-195 in the adsorption process was examined at initial dye concentration of 10-160 mg/L, and the result is given in Fig. 6.

Table 2. Parameters of the three kinetic models for RY-176 and RR-195 adsorption by ABWS-800.

Dye	C_0 (mg/L)	Pseudo-first-order			Pseudo-second-order			Elovich		
		$q_{e,cal}$	k_1	R^2	$q_{e,cal}$	k_2	R^2	α	β	R^2
RY-176	100	7.394	0.005	0.947	19.455	0.003	0.998	41.324	0.478	0.962
	25	2.751	0.006	0.941	7.013	0.008	0.999	16.475	1.363	0.983
RR-195	100	3.968	0.005	0.901	26.247	0.006	0.999	7.44E+06	0.836	0.982
	25	1.976	0.005	0.937	7.305	0.010	0.990	441.801	1.793	0.952

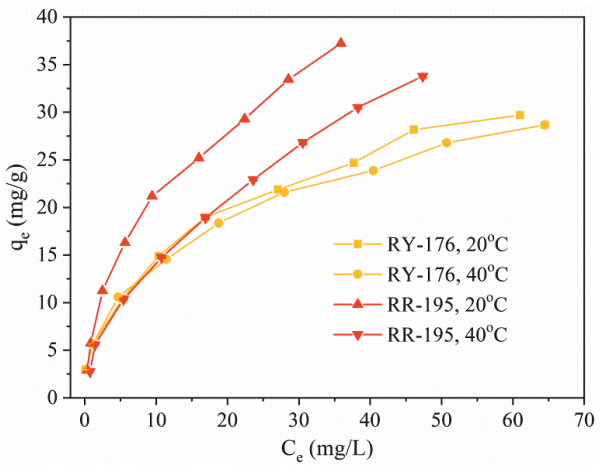

Fig. 6. The influence of equilibrium concentration in the adsorption process of RY-176 and RR-195 by ABWS-800 (pH: 5.5, Reaction time: 8 h).

As seen in Fig. 6, the adsorption capacity of the two dyes increased as equilibrium concentration improved, accompanying with a decrease in the adsorption rate, indicating the gradual saturation of surface active sites on ABWS-800. Between the temperatures applied in the adsorption experiment, low temperature (20°C) was more beneficial for the removal of the two dyes, especially for RR-195, suggesting that the adsorption of the two active dyes onto ABWS-800 was exothermic. It could be explained on the basis that the solubility of the dyes increased at higher temperature and adsorbate-adsorbent interactions decreased, thus resulting in decreased adsorption. The results also indicate that more desorption than adsorption of the two dyes took place at higher temperature [45]. Consideration of the high temperature properties of dye wastewater, it would be not in favorable to the application of ABWS-800 to the decontamination of dyes wastewater.

The equilibrium isotherm is crucial to understand the interaction between adsorbate and adsorbent. The Langmuir and Freundlich isotherms, expressed as Eq. (5) and Eq. (6), respectively, were used to characterize the adsorption of RY-176 and RR-195 onto ABWS-800.

$$\frac{c_e}{q_e} = \frac{1}{q_m b} + \frac{c_e}{q_m} \tag{5}$$

$$\log q_e = \log k_f + \frac{1}{n} \log c_e \tag{6}$$

where c_e (mg/L), q_e (mg/g) and q_m (mg/g) is the concentration, adsorption capacity and the maximum adsorption capacity at equilibrium, respectively. b (L/mg) is the Langmuir constant, k_f ((mg/g)/(mg/L)^n) and n are the Freundlich constant.

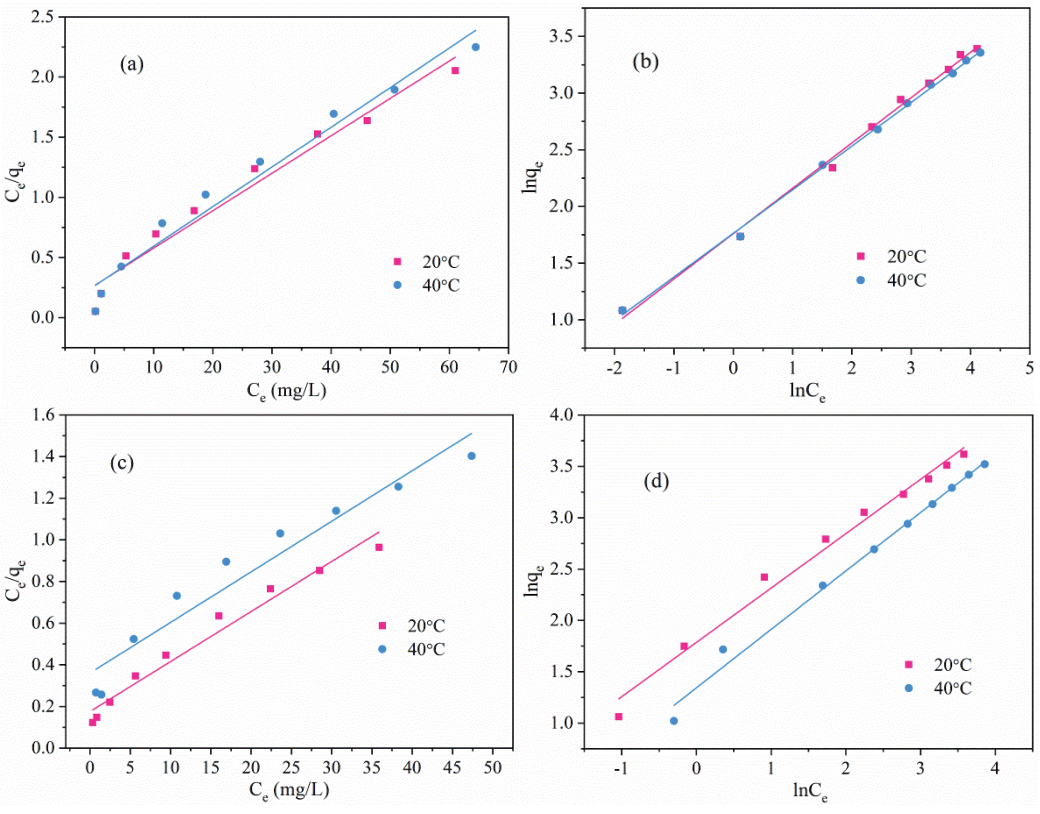

Fig. 7. The fitting results of the two isotherms. a) Langmuir isotherm model, RY-176; b) Freundlich isotherm model, RY-176; c) Langmuir isotherm model, RR-195; d) Freundlich isotherm model, RR-195.

Table 3. Parameters of Langmuir and Freundlich isotherms for the adsorption of RY-176 and RR-195 by ABWS-800.

Dye	Temperature (ºC)	Langmuir		Freundlich		
		q_m	R^2	k_f	n	R^2
RY-176	20	32.154	0.971	81.581	2.501	0.995
	40	30.395	0.971	96.075	2.595	0.998
RR-195	20	41.494	0.971	29.214	1.889	0.987
	40	41.152	0.940	7.037	1.451	0.991

The fitting results and the parameters of adsorption isotherms are presented and summarized in Fig. 7 and Table 3, respectively.

As shown in Table 3, the higher R^2 values of Freundlich isotherm at both of the two temperatures than those of Langmuir isotherm for the adsorption of RY-176 and RR-195 by ABWS-800 indicated that the Freundlich equation was more suitable to describe the adsorption process, which presented that the heterogeneous surface of ABWS-800 and multilayer adsorption with non-uniform distribution of heat energy on ABWS-800 surface occurred [46]. The value of 1/n which varied between 0.39 and 0.69, indicating the favorable adsorption of dye molecule onto ABWS-800 and chemical adsorption took place during the removal of the two dyes [32]. The higher k_f value for RR-195 demonstrated that RR-195 had a higher adsorption affinity to the surface of ABWS-800 compared with RY-176, thus resulting in a greater adsorption capacity for RR-195, which was identified with the results reported in the previous section.

Effect of Salt Concentration

The effect of Na_2SO_4 on adsorption of RY-176 and RR-195 by ABWS-800 was investigated since Na_2SO_4 is widely used to improve the reactive dye uptake during the dyeing process. The result is shown in Fig. 8.

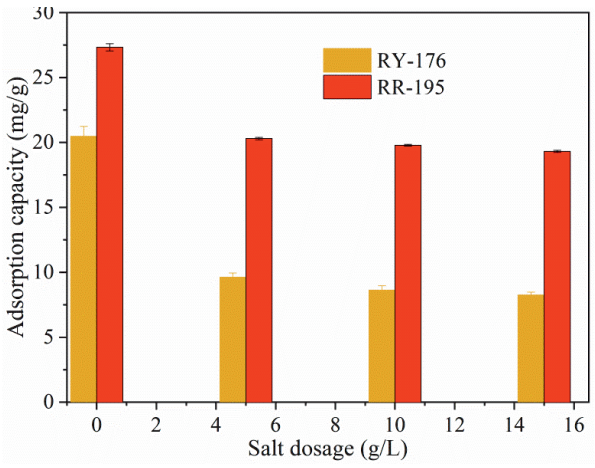

Fig. 8. Effect of salt concentration on adsorption of RY-176 and RR-195 by ABWS-800 (Reaction time: 3 h, pH: 5.5, Temperature: 30ºC).

As shown in Fig. 8, the removal of the two reactive dyes by ABWS-800 was inhibited clearly in the presence of Na_2SO_4. The adsorption capacity of RY-176 and RR-195 decreased from 20.5mg/g and 27.3 mg/g to 9.6 mg/g and 20.3 mg/g, respectively, as Na_2SO_4 dosage increased from 0 to 5 g/L, and further deceased to 8.3 mg/g and 19.3 mg/g, respectively, as Na_2SO_4 dosage increased to 15 g/L. The results indicated that the presence of Na_2SO_4 imposed more significant impact on the adsorption of RY-176 and RR-195 than the increase of Na_2SO_4 concentration. The result in the present study agreed well with that reported in the literature. According to Netpradit [36], a high decrease in reactive dyes adsorption by metal hydroxide sludge occurred in the presence of Na_2SO_4, which had higher valence, would compete strongly with SO_3^{2-} for binding sites on adsorbent. Moreover, the adsorption of SO_4^{2-} might also block some of the adsorption active sites for the dyes molecules, consequently leading to the decrease in the adsorption of the two dyes on ABWS-800.

Conclusions

In this study, the enhanced removal of two reactive dyes, RY-176 and RR-195, by ABWS modified by calcination was examined. Calcination was proved to be an effective way to improve the adsorption capacity of Al-based waterworks sludge, and 800ºC was found to be the best calciantion temperature in the range of 200-900ºC. The results of the adsorption experiment indicated that solution pH impacted slightly on the adsorption of the two dyes by ABWS-800. Compared with the first-second-order model and Elovich model, the pseudo-second-order kinetic model was better to describe the adsorption process, and Freundlich isotherm model fitted the experimental data better than the Langmuir isotherm model. The adsorption of both the two dyes on ABWS-800 was suppressed clearly by Na_2SO_4. The study indicates that ABWS can be a potential adsorbent for dye-bearing wastewater treatment. However, it is necessary to assess the reusability of ABWS. Meanwhile, granules or pellet can be made from the powder ABWS to improve its separability and applicability.

Acknowledgment

The authors wish to express gratefully acknowledge for the funding support from the Scientific Research Foundation of North China University of Water Resources and Electric Power (No. 40001) and the assistance from Zhongzhou water holding Co., Ltd in sampling.

Conflict of Interest

The authors declare no conflict of interest.

References

1. CELIK S., DUMAN N., SAYIN F., TUNALI AKAR S., AKAR T. Microbial cells immobilized on natural biomatrix as a new potential ecofriendly biosorbent for the biotreatment of reactive dye contamination. J. Water Process Eng. **39**, 101731, **2021**.
2. ZHANG H., WANG J., XIE K., PEI L., HOU A. Synthesis of novel green reactive dyes and relationship between their structures and printing properties. Dyes Pigments. **174**, 108079, **2020**.
3. WEI Y., CHENG X., DING A., XU J. Magnesium Silicate Polymer as a Coagulant for Reactive Dye Removal from Wastewater: Considering the Intrinsic pH in Magnesium Silicate Polymer and Coagulation Behavior. ACS Omega. **5**, 26094, **2020**.
4. GOWRI R., VIJAYARGHAVAN R., MEENAMBIGAI P. Microbial degradation of reactive dyes-A Review. Int. J. Curr. Microbiol. Appl. Sci. **3**, 421, **2014**.
5. SANTOS D.H.S., DUARTE J.L.S., TAVARES M.G.R., TAVARES M.G., FRIEDRICH L.C., MEILI L., PIMENTEL W.R.O., TONHOLO J., ZANTA C.L.P.S. Electrochemical degradation and toxicity evaluation of reactive dyes mixture and real textile effluent over DSA® electrodes. Chem. Eng. Process. **153**, 107940, **2020**.
6. ALMEIDA C.A.P., DEBACHER N.A., DOWNS A.J., COTTET L., MELLO C.A.D. Removal of methylene blue from colored effluents by adsorption on montmorillonite clay. J. Colloid Interf. Sci. **332**, 46, **2009**.
7. GAUTAM D., SAYA L., HOODA S. Fe_3O_4 loaded chitin - A promising nano adsorbent for Reactive Blue 13 dye. Environ. Adv. **2**, 100014, **2020**.
8. MORADI H., SHARIFNIA S., RAHIMPOUR F. Photocatalytic decolorization of reactive yellow 84 from aqueous solutions using ZnO nanoparticles supported on mineral LECA. Mater. Chem. Phys. **158**, 38, **2015**.
9. LIU S., LI B., QI P., YU W., ZHAO J., LIU Y. Performance of Freshly Generated Magnesium Hydroxide (FGMH) for Reactive Dye Removal. Colloid Interfac. Sci. **28**, 34, **2019**.
10. MCYOTTO F., WEI Q., MACHARIA D.K., HUANG M., SHEN C., CHOW C.W.K. Effect of dye structure on color removal efficiency by coagulation. Chem. Eng. J. **405**, 126674, **2021**.
11. DEĞERMENCI G.D., DEĞERMENCI N., AYVAOĞLU V., DURMAZ E., ÇAKIR D., AKAN E. Adsorption of reactive dyes on lignocellulosic waste; characterization, equilibrium, kinetic and thermodynamic studies. J. Clean. Prod. **225**, 1220, **2019**.
12. DE LA LUZ-ASUNCIÓN M., PÉREZ-RAMÍREZ E.E., MARTÍNEZ-HERNÁNDEZ A.L., GARCÍA-CASILLAS P.E., LUNA-BÁRCENAS J.G., VELASCO-SANTOS C. Adsorption and kinetic study of Reactive Red 2 dye onto graphene oxides and graphene quantum dots. Diam. Relat. Mater. **109**, 108002, **2020**.
13. TIE J. X., CHEN D., ZHAO M. Q., WANG X. L., ZHOU S. G., PENG L. G.Adsorption of reactive green 19 from water using polyaniline/bentonite. J. Water Reuse Desal. **6**, 515, **2016**.
14. ARSHAD R., BOKHARI T.H., JAVED T., BHATTI I.A., RASHEED S., IQBAL M., NAZIR A., NAZ S., KHAN M.I., KHOSA M.K.K., IQBAL M., ZIA-UR-REHMAN M. Degradation product distribution of Reactive Red-147 dye treated by UV/H2O2/TiO2 advanced oxidation process. J. Mater. Res. Technol. **9**, 3168, **2020**.
15. HOMEM N. C., DE CAMARGO LIMA BELUCI N., AMORIM S., REIS R., VIEIRA A. M. S., VIEIRA M. F., BERGAMASCO R., AMORIM M. T. P. Surface modification of a polyethersulfone microfiltration membrane with graphene oxide for reactive dyes removal. Appl. Surf. Sci. **486**, 499, **2019**.
16. PRABHAKAR Y., GUPTA A., KAUSHIK A. Microbial degradation of reactive red-35 dye: Upgraded progression through Box–Behnken design modeling and cyclic acclimatization. J. Water Process Eng. **40**, 101782, **2021**.
17. SHI S.Q, YANG J.K., LIANG S., LI M.G., GAN Q., XIAO K.K., HU J.P. Enhanced Cr (VI) removal from acidic solutions using biochar modified by Fe_3O_4@ SiO_2-NH_2 particles. Sci. Total Environ. **628**, 499, **2018**.
18. ABDEL AZEEM S.M., ATTAF S.M., EI-SHAHAT M.F. Solid-phase extraction of Cu, Zn, and Mn from Nile river and tap water prior to flame atomic absorption determination. Desalin. Water Treat. **57**, 21893, **2016**.
19. ALOTHMAN Z.A. A review: fundamental aspects of silicate mesoporous materials. Materials. **5**, 2874, **2012.**
20. KHAN M.A., ALQADMI A.A., WABAIDUR S.M., SIDDIQUI M.R., JEON B.H., ALSHAREEF S.A., ALOTHMANl Z.A., HAMEDELNIEL A.E. Oil industry waste based non-magnetic and magnetic hydrochar to sequester potentially toxic post-transition metal ions from water. J. Hazard. Mater. **400**, 123247, **2020**.
21. ALI I., ALHARBI O.M., ALOTHMANZ A., AL-MOHAIMEED A.M., ALWARTHAN A. Modeling of fenuron pesticide adsorption on CNTs for mechanistic insight and removal in water. Environ. res. **170**, 389, **2019**.
22. ALQADAMI A.A., KHAN M.A., SIDDIQUIi M.R., ALOTHMANl Z.A. Development of citric anhydride anchored mesoporous MOF through post synthesis modification to sequester potentially toxic lead (II) from water. Micr. Mesopor. Mat. **261**, 198, **2018.**
23. ALOTHMAN Z.A., WABAIDUR S.M. Application of carbon nanotubes in extraction and chromatographic analysis: A review. Arab. J. Chem. **12**, 633, **2019**.
24. WABAIDUR S.M., KHAN M.A., SIDDIQUI M.R., OTERO M., JEON B.H., ALOTHMAN Z.A., HAKAMI A.A.H. Oxygenated functionalities enriched MWCNTs decorated with silica coated spinel ferrite–A nanocomposite for potentially rapid and efficient de-colorization of aquatic environment. J. Mol. Liq. **317**, 113916, **2020**.
25. TIE J.X., FANG X.H., WANG X.L., ZHANG Y., LI G. T., TANG D.Y. Adsorptive removal of a reactive azo dye using polyaniline-intercalated bentonite. Pol. J. Environ. Stud. **26**, 1259, **2017**.

26. KHAN M.A., WABAIDUR S.M., SIDDIQUIi M.R., ALQADAMI A.A., KHAN A.H. Silico-manganese fumes waste encapsulated cryogenic alginate beads for aqueous environment de-colorization. J. Clean. Prod. **244**, 118867, **2020**.
27. KENAWY E.R., GHFAR A.A., WABAIDUR S.M., KHAN M.A., SIDDIQUI M.R., ALOTHMAN Z.A., ALQADAMIl A.A, HAMID M. Cetyltrimethylammonium bromide intercalated and branched polyhydroxystyrene functionalized montmorillonite clay to sequester cationic dyes. J. Environ.Manag. **219**, 285, **2018.**
28. ALI I., ALHARBI O.M., ALOTHMAN Z.A., BADJAH A.Y. Kinetics, thermodynamics, and modeling of amido black dye photodegradation in water using Co/TiO_2 nanoparticles. Photochem. Photobiol. **94**, 935, **2018.**
29. AL-TAHMAZI T., BABATUNDE A.O. Mechanistic study of P retention by dewatered waterworks sludges. Environ. Technol. Inno. **6**, 38, **2016**.
30. HOU Q., MENG P., PEI H., HU W., CHEN Y. Phosphorus adsorption characteristics of alum sludge: Adsorption capacity and the forms of phosphorus retained in alum sludge. Mater. Lett., **229**, 31, **2018**.
31. SHEN C., ZHAO Y., LI W., YANG Y., LIU R., MORGEN D. Global profile of heavy metals and semimetals adsorption using drinking water treatment residual. Chem. Eng. J. **372**, 1019, **2019**.
32. ZHAO X., LUO H., TAO T., ZHAO Y. Immobilization of arsenic in aqueous solution by waterworks alum sludge: prospects in China. Int. J. Environ. Stud. **72**, 989, **2015**.
33. KAYRANLI B. Adsorption of textile dyes onto iron based waterworks sludge from aqueous solution; isotherm, kinetic and thermodynamic study. Chem. Eng. J. **173**, 782, **2011**.
34. JEON E.K., RYU S., PARK S.W., WANG L., TSANG D.C.W., BAEK K. Enhanced adsorption of arsenic onto alum sludge modified by calcination. J. Clean. Prod. **176**, 54, **2018**.
35. EVERAERT M., BERGMANS J., BROOS K., HERMANS B., MICHIELSEN B. Granulation and calcination of alum sludge for the development of a phosphorus adsorbent: From lab scale to pilot scale, J. Environ. Manag. **279**, 111525, **2021**.
36. ALOTHMAN Z.A., BAHKAHI ALI H., KHIYAMI M.A., ALFADUL S.M., WABAIDUR S.M., ALAM M., ALFARHAN B.Z., Low cost biosorbents from fungi for heavy metals removal from wastewater, Sep. Sci. Technol. **55**, 1766, **2020**.
37. WANG T., LIU H., DUAN C., XU R., ZHANG Z., SHE D., ZHENG J. The eco-friendly biochar and valuable bio-oil from Caragana korshinskii: Pyrolysis preparation, characterization, and adsorption applications. Mater. **13**, 3391, **2020**.
38. ZHANG R.L., WANG J.R., MA D.L. Structural Investigations of Sol-Gel Prepared Bi_2O_3-$AlPO_4$-SiO_2 Glasses by Solid State Nuclei Magnetic Resonance Spectroscopy. J. Chin. Ceram. Soc. **50**, 913, **2022**.
39. XU X., HU X., DING Z., GAO B. Sorption of aqueous methylene blue, cadmium and lead onto biochars derived from scrap papers. Pol. J. Environ. Stud. **29**, 4409, **2020**.
40. WANG X., PFEIFFER H., WEI J., WANG J., ZHANG J. Fluoride ions adsorption from water by $CaCO_3$ enhanced Mn-Fe mixed metal oxides. Front. Chem. Sci. Eng. 1-13, **2022**.
41. NETPRADIT S., THIRAVETYAN P., TOWPRAYOON S. Adsorption of three azo reactive dyes by metal hydroxide sludge: effect of temperature, pH, and electrolytes. J. Colloid Interf. Sci. **270**, 255, **2004**.
42. NETPRADIT S., THIRAVETYAN P., TOWPRAYOON S. Application of 'waste' metal hydroxide sludge for adsorption of azo reactive dyes. Water Res. **37**, 763, **2003**.
43. SAREMI F., MIROLIAEI M.R., NEJAD M.S., SHEIBANI H. Adsorption of tetracycline antibiotic from aqueous solutions onto vitamin B6-upgraded biochar derived from date palm leaves. J. Mol. Liq. **318**, 114126, **2020**.
44. KANG S., PARK S.M., PARK J.G., BAEK K. Enhanced adsorption of arsenic using calcined alginate bead containing alum sludge from water treatment facilities. J. Environ. Manage. **234**, 181, **2019**.
45. IQBAL M.J., ASHIQ M.N. Adsorption of dyes from aqueous solutions on activated charcoal. J. Hazard. Mater. **139**, 57, **2007**.
46. JAAFARI J., BARZANOUNI H., MAZLOOMI S., FARAHANI A.A., HAGHIGHAT G.A. Effective adsorptive removal of reactive dyes by magnetic chitosan nanoparticles: Kinetic, isothermal studies and response surface methodology. Int. J. Biol. Macromol. **164**, 344, **2020**.